



# Influence of the catalytic support on the industrial Fischer–Tropsch synthetic diesel production

A.R. de la Osa\*, A. De Lucas, A. Romero, J.L. Valverde, P. Sánchez

Chemical Engineering Department, Faculty of Chemistry, University of Castilla La Mancha, Avda. Camilo José Cela 12, 13071 Ciudad Real, Spain

## ARTICLE INFO

### Article history:

Received 28 September 2010

Received in revised form

30 November 2010

Accepted 2 December 2010

Available online 12 January 2011

### Keywords:

Fischer–Tropsch synthesis

Cobalt catalyst

Alumina

Bentonite

Titania

Silicon carbide

## ABSTRACT

A range of cobalt catalysts supported on alumina, titania, bentonite and the newer silicon carbide was examined for catalytic activity and product selectivity in the Fischer–Tropsch reaction. Experiments were carried out on a bench scale fixed bed reactor. TPR results showed that Co/TiO<sub>2</sub> and Co/bentonite were easier to reduce than Co/Al<sub>2</sub>O<sub>3</sub> and Co/SiC based catalyst. Particle size depended on nature of support and specific area. Catalyst Co/SiC provided good catalytic results at temperatures higher than 235 °C whereas Co/bentonite showed high catalytic activity at low temperatures. However, Co/bentonite was found to enhance the formation of oxygenated compounds. Hydrocarbon distribution was influenced by the support. Co/Al<sub>2</sub>O<sub>3</sub> shifted to lighter hydrocarbon than Co/TiO<sub>2</sub> and Co/bentonite. Co/SiC yielded to higher molecular weight hydrocarbons products distribution as compared with Co/alumina catalyst.

© 2010 Elsevier B.V. All rights reserved.

## 1. Introduction

The depletion of fossil energy reserves, and the need for reduction of greenhouse gas emissions, mainly CO<sub>2</sub>, makes renewable energy sources very attractive [1]. Coal gasification is a well established technology to produce syngas capable of being compatible with biomass as feedstock [2]. Co-gasification of biomass with coal, could contribute to the reduction of both fossil fuels dependency and CO<sub>2</sub> emissions. ELCOGAS (Spain) is an integrated gasification combined cycle plant, IGCC, which has participated in a project for co-gasification of coal/petcoke and exhausted olive husk where biosyngas was demonstrated to be feasible to produce. An attractive alternative for production of clean, sustainable and renewable automotive fuels from gasified carbon-biomass is the Fischer–Tropsch synthesis (FTS) [3–5].

Cobalt based catalysts have been widely used for FTS due to their high selectivity to linear paraffins, low water–gas shift activity and stability toward deactivation by water [6]. In FT process, it was found that the catalytic activity and selectivity were influenced by nature and structure of support, metal dispersion, metal loading, and/or preparation method [7]. Most studies on FT catalysts have been carried out with metals supported on silica, alumina or titania [8]. Also, other supports such as carbon in the form of activated

carbon and carbon nanotubes (CNTs) have been investigated in the FTS [9–12]. However, silicon carbide has never been used for this purpose. Silicon carbide is one of the most advanced ceramic materials for its remarkable chemical and thermomechanical properties [13].

The aim of the present work was to study the influence of different supports, including the newer silicon carbide, on the activity and diesel product selectivity of cobalt-based Fischer–Tropsch catalysts, using a bench-scale experimental device.

## 2. Experimental

### 2.1. Bench scale set-up description

The facility which is fully automated and computerized consists of three physically separated parts: feed gas and mixing supply system, reaction system and products analysis system.

N<sub>2</sub>, H<sub>2</sub> and CO (high purity supplied by PRAXAIR) are fed as the main gases. Each of these gases can be fed through two separate lines that have the same elements but different flow rate. The bench scale set-up included an Inconel fixed bed reactor (17.7 mm ID and 1000 mm length) for FT experiments.

The gaseous effluent was connected to the input of a gas chromatograph by means of a Peltier cell. The analysis system consisted of both gas analysis system and liquid analysis system. The first one consisted of a MicroGC (CP-4900 Micro-GC VARIAN) with two analysis columns (Molsieve 5A for H<sub>2</sub>, N<sub>2</sub>, CH<sub>4</sub> and CO and Pora Pack

\* Corresponding author. Tel.: +34 926 29 53 00x3509; fax: +34 926 29 52 56.  
E-mail addresses: [AnaRaquel.Osa@uclm.es](mailto:AnaRaquel.Osa@uclm.es), [anraquel@gmail.com](mailto:anraquel@gmail.com) (A.R. de la Osa).

Q column for CO<sub>2</sub>, ethane and propane) using Ar and He as carrier gases, respectively. The liquid product distribution was measured by using a GC–FID (Trace GC Ultra (ThermoFisher Scientific)), which included an ultrafast capilar microcolumn.

## 2.2. Catalyst preparation

Catalyst Co/support was prepared by incipient wetness impregnation. All the supports  $\gamma$ -Al<sub>2</sub>O<sub>3</sub> (Merck), Na-bentonite (Fisher), TiO<sub>2</sub> (Merck) and SiC (Sicat Catalysts) were impregnated with an aqueous solution of cobalt nitrate hexahydrate (Merck) using two-steps incipient wetness to give a final catalyst with 15 wt.% cobalt. After each impregnation, the catalyst was dried at 120 °C for 2 h. After the last impregnation and drying, the catalyst was calcined at 550 °C for 6 h. Then, Co/ $\gamma$ -alumina, Co/bentonite and Co/titania powder were pelletized and transform into irregular particles of 2 mm size whereas Co/silicon carbide was used in extrudate form of 2 mm.

## 2.3. Catalyst characterization

In order to quantify the total amount of metal into the catalyst, atomic absorption (AA) measurement ( $\pm 1\%$  error), was made by using a SPECTRAA 220FS analyzer. Surface area/porosity measurements ( $\pm 3\%$  error), were conducted using a Micromeritics ASAP 2010 sorptometer apparatus with N<sub>2</sub> (at 77 K) as sorbate. The total specific surface areas were determined by the multi-point BET method and pore size distributions were evaluated using the standard BJH treatment [14]. XRD patterns were determined by a Philips model X'Pert MPD with Co-filtered Cu K $\alpha$  radiation ( $\lambda = 1.54056 \text{ \AA}$ ). The average crystallite size of Co<sub>3</sub>O<sub>4</sub> was calculated according to Scherrer's equation [15]. Dispersion was calculated from particle size measured by XRD according to the formula reported by Jones [16]. TPR measurements of the catalysts were carried out with an Autochem HP 2950 analyzer ( $\pm 2\%$  error), under an argon/hydrogen flow (83/17 volumetric ratio). The temperature and detector signal were then continuously recorded while heating at 10 °C min<sup>-1</sup> up to 900 °C. The intrinsic basicity of each catalyst was determined by CO<sub>2</sub> temperature programmed desorption (CO<sub>2</sub>-TPD) analysis in the same system as used in TPR analysis ( $\pm 3\%$  error). The sample was firstly reduced by heating at 5 °C min<sup>-1</sup> under a flow of hydrogen/argon. After cooling to 50 °C under flow of helium, CO<sub>2</sub> was fed at a rate of 30 ml min<sup>-1</sup> for 30 min. Later, the sample was purged with helium for 1 h in order to eliminate physisorbed species. The temperature was ramped at 10 °C min<sup>-1</sup> from 50 to 900 °C. Then, CO<sub>2</sub>-TPD data were acquired. The extent of reduction was determined by pulse oxidation with O<sub>2</sub> of reduced samples at 400 °C in the same apparatus as used for the TPR experiments. After reduction, the sample was kept at 400 °C in He and held for 1 h to desorb any chemisorbed H<sub>2</sub>. Calibrated pulses of O<sub>2</sub> were then added into the continuous He flow until no further consumption of O<sub>2</sub> was detected by the thermal conductivity detector located downstream of the reactor. The extent of reduction was calculated assuming stoichiometric reoxidation of Co<sup>0</sup> to Co<sub>3</sub>O<sub>4</sub>.

## 2.4. Activity test

Fischer–Tropsch synthesis was performed under 20 bars, which is an operating pressure representative of the pressurized gasification industrial process. A weighed sample of catalyst (5 g) was packed in the reactor between layers of inert material (SiC). Prior to Fischer–Tropsch synthesis, catalysts Co/bentonite and Co/TiO<sub>2</sub> were pretreated with pure H<sub>2</sub> at 350 °C (heating rate 5 °C min<sup>-1</sup>) for 2 h whereas catalysts Co/Al<sub>2</sub>O<sub>3</sub> and Co/SiC needed 550 °C (heating rate 5 °C min<sup>-1</sup>) for 2 h. After reduction, the catalyst was flushed

with N<sub>2</sub> at 220 °C getting pressure rise up to 20 bars. Catalytic activity has been studied in the temperature range of 220–300 °C for 10 h. Gas hourly space velocity (GHSV) was set on 6000 h<sup>-1</sup> and H<sub>2</sub>/CO molar ratio was kept at 2. Effluent gas compositions were analyzed online, at 1.5 h intervals for 12 h whereas effluent liquid compositions were analyzed once operating conditions remained stable (after 6–8 h).

## 3. Results and discussion

Activity and hydrocarbon selectivity of cobalt supported on alumina, titania, bentonite and silicon carbide are summarized in Table 1. Results revealed that catalytic CO conversion seemed to be deeply dependent on increasing reaction temperature. Hence, an increase of the reaction temperature resulted in a gradually increase in selectivity to CO<sub>2</sub>, C<sub>1</sub>–C<sub>4</sub> fraction and CO conversion, whereas C<sub>5</sub><sup>+</sup> fraction was diminished. As reported by Farias et al. and Tian et al. [17,18], it was found that higher temperatures promote CO dissociation and provide more surface C atoms leading to the release of hydrocarbons. Moreover, methane formation was also favoured owing to H<sub>2</sub>/CO ratio enrichment inside the reactor with increasing reaction temperature [17–19]. With regard to the hydrocarbon distribution and accordingly to Ngantsoue and coworkers [20], the fraction of alkenes, especially C<sub>2</sub>, decreased as the CO conversion increased. This observation was consistent with those previously reported indicating that at higher reaction temperatures, olefins are preferentially hydrogenated and chain propagation was suppressed [21,22].

The order of increasing CO hydrogenation activity at temperatures higher than 235 °C for the catalysts containing 10–13 wt.% of cobalt was Co/TiO<sub>2</sub> < Co/Al<sub>2</sub>O<sub>3</sub> < Co/bentonite < Co/SiC. The same trend was observed for CO rate and FTS rate. As reported elsewhere [23], the FTS rate and CO conversion are strongly dependent and proportional to the number of surface reduced active cobalt sites. Catalysts Co/bentonite and Co/TiO<sub>2</sub> showed a wide single TPR reduction peak (Fig. 1) which was related to the complete reduction of Co<sub>3</sub>O<sub>4</sub> to Co<sup>0</sup>. However, multiple reduction peaks were observed for catalyst Co/Al<sub>2</sub>O<sub>3</sub> and Co/SiC. The first peak was ascribed to the reduction of Co<sub>3</sub>O<sub>4</sub> to CoO, followed by the second peak that corresponded to the reduction of CoO to Co. Hydrogen consumption occurring at temperatures larger than 450 °C may be assigned to the reduction of either cobalt silicates or cobalt aluminates [24,25]. As explained in Section 2.4, 350 °C and 550 °C were chosen as temperatures that provide complete reduction of each catalyst, respectively. Thus, accordingly to this trend, catalyst Co/SiC resulted in the highest percentage of reduction measured by pulse oxidation technique.

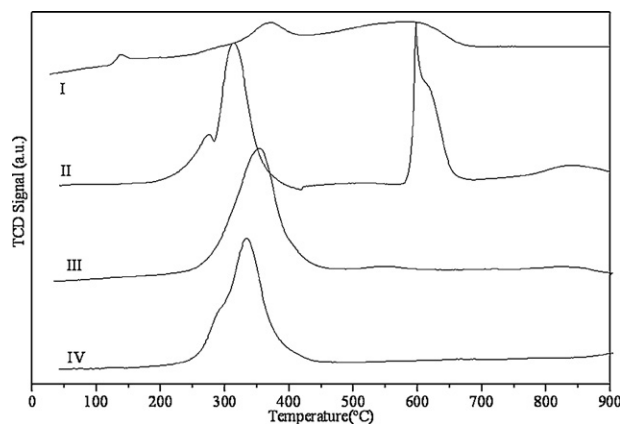


Fig. 1. TPR profiles: (I) Co/Al<sub>2</sub>O<sub>3</sub>, (II) Co/SiC, (III) Co/bentonite and (IV) Co/TiO<sub>2</sub> catalysts.

**Table 1**  
Catalysts characterization and catalytic activity.

Sample	wt.% Co	BET area (m <sup>2</sup> g <sup>-1</sup> )	Dpore (nm)	Total pore volume (cm <sup>3</sup> g <sup>-1</sup> )	dCo <sub>3</sub> O <sub>4</sub> (nm) (XRD)	% Reduction (O <sub>2</sub> pulse)	D (%) (XRD)	Weak basicity (mmol g <sup>-1</sup> )	Strong basicity (mmol g <sup>-1</sup> )	
Chemical composition and physical properties of FTS catalysts										
Co/Al <sub>2</sub> O <sub>3</sub>	11	90.1	6.0	0.136	30.7	48.6	4.2	0.165	0.066	
Co/bentonite	13	9.6	19.1	0.046	106.1	40.4	1.2	0.077	0.086	
Co/TiO <sub>2</sub>	13	9.4	8.6	0.020	85.6	45.6	1.5	0.026	0.016	
Co/SiC	10	21.5	7.2	0.039	45.0	79.0	2.8	0.002	0.029	
Catalyst	T (°C)	CO rate (mol/molCo.h)	FTS rate (mol/molCo.h)	CO <sub>2</sub> rate (mol/molCo.h)	Xco (%)	Hydrocarbon selectivity (%)				
						CO <sub>2</sub>	C <sub>1</sub> -C <sub>4</sub>	O/O+P (C <sub>2</sub> )	O/O+P (C <sub>3</sub> )	C <sub>5</sub> <sup>+</sup>
Catalytic activity. GHSV: 6000 h <sup>-1</sup> . H <sub>2</sub> /CO: 2										
Co/Al <sub>2</sub> O <sub>3</sub>	220	5.98	5.93	0.04	13.9	0.70	15.08	0.46	0.95	84.22
	228	9.93	9.81	0.11	23.1	1.16	9.14	0.24	0.85	89.70
	235	8.76	8.65	0.11	20.4	1.29	13.66	0.28	0.89	85.05
	242	13.24	12.85	0.39	30.8	2.95	19.07	0.20	0.82	77.98
	250	17.44	16.92	0.52	40.6	2.99	21.52	0.15	0.77	75.49
	300	34.07	28.38	3.66	79.4	12.93	39.48	0.03	0.57	47.59
Co/bentonite	220	20.81	20.79	0.02	57.3	0.08	0.26	0.12	1.00	99.66
	228	23.26	23.24	0.02	64.1	0.09	0.17	0.08	0.69	99.74
	235	22.04	22.02	0.02	60.7	0.09	0.15	0.00	0.71	99.76
	242	23.89	23.86	0.03	65.8	0.14	0.09	0.00	0.93	99.79
	250	24.54	24.50	0.04	67.6	0.16	0.41	0.00	0.52	99.43
	300	28.48	28.39	0.09	78.4	0.33	2.82	0.00	0.04	96.85
Co/TiO <sub>2</sub>	220	1.29	1.28	0.01	3.4	1.05	7.02	0.53	1.00	92.69
	228	2.08	2.06	0.02	5.5	1.03	9.58	0.44	1.00	89.39
	235	2.51	2.41	0.10	6.7	4.03	13.62	0.31	0.95	82.35
	242	3.64	3.54	0.10	9.4	3.45	13.93	0.22	0.93	82.62
	250	2.97	2.87	0.10	7.9	3.53	14.76	0.18	0.93	81.71
	300	23.0	22.4	0.58	60.8	2.63	26.76	0.03	0.66	70.60
Co/SiC	220	3.49	3.47	0.02	7.4	0.47	6.20	0.36	1.00	93.33
	228	5.73	5.69	0.04	12.1	0.66	2.88	0.33	1.00	96.46
	235	31.71	31.5	0.21	67.2	0.65	5.29	0.09	0.73	94.06
	242	34.12	33.8	0.32	72.1	0.93	6.30	0.06	0.64	92.78
	250	35.22	34.81	0.41	74.9	0.65	9.31	0.10	0.72	90.04
	300	37.42	36.78	0.64	79.2	1.71	15.73	0.05	0.71	82.56

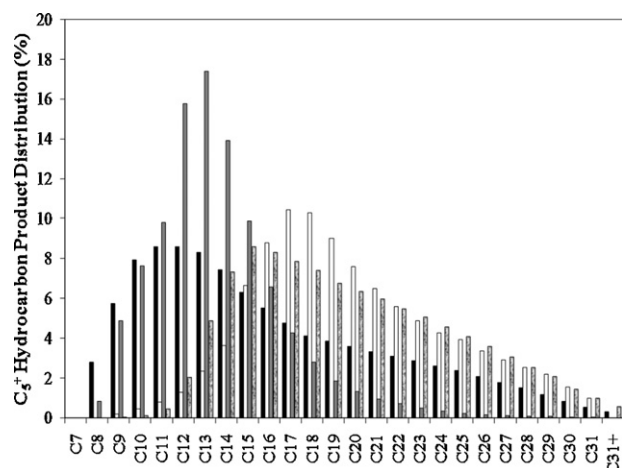


Fig. 2. Influence of support on  $C_5^+$  product distribution. Reaction temperature: 250 °C. (■) Co/Al<sub>2</sub>O<sub>3</sub>, (▒) Co/SiC, (□) Co/bentonite, (□) Co/TiO<sub>2</sub>.

It was also found [23] that Co particle size was related to the basic behaviour of catalyst, suggesting a direct proportionality between surface basicity and hydrogenation rate. Table 1 shows Co<sub>3</sub>O<sub>4</sub> particle sizes and intrinsic basicity attributed to each catalyst (measured by CO<sub>2</sub>-TPD analysis). In this study, there was no clear correlation between particle size and basic behaviour of catalysts. Thus, textural properties of the support could be responsible of the differences on metal deposition. The N<sub>2</sub> adsorption/desorption isotherm associated to Co/Al<sub>2</sub>O<sub>3</sub> can be accounted for as a type IV reference isotherms whereas Co/TiO<sub>2</sub>, Co/bentonite and Co/SiC agreed with a conjunction of type II and type IV, according to the IUPAC classification. The specific surface area increased in the order of Co/TiO<sub>2</sub> ≤ Co/bentonite < Co/SiC < Co/Al<sub>2</sub>O<sub>3</sub>, however, the average pore size is found to be smallest on Co/Al<sub>2</sub>O<sub>3</sub> catalyst. The mono-modal pore size distribution of all catalysts revealed a uniform distribution of cobalt species on each support. Moreover, particle size revealed deposition of large cobalt particles on the outer surface of the support.

It was important to note that among catalysts with low specific area, catalyst Co/bentonite seemed to be influenced in a lesser extent by reaction temperature, showing higher FTS activity and  $C_5^+$  selectivity. However, the surprisingly higher activity exhibited by this catalyst at low temperatures could not be only explained in terms of dispersion and reduction (Table 1); even when Na<sup>+</sup> present in bentonite support was considered to improve reduction and dispersion leading to an enhanced adsorption of carbon monoxide [26] and growth probability [27]. Then, a further study should be performed in order to find a better explanation. Furthermore, since the liquid products recovered did not match with the expected one and a small fraction of methanol and ethanol was found in the aqueous phase (measured by means of gas chromatography (Younglin YL-6100 GC with a FID detector)), Co/bentonite was supposed to provide oxygenated compounds that are easily evaporated [28].

Fig. 2 illustrates the comparison of the catalysts demonstrating that support clearly influences  $C_5^+$  FTS product distribution. Hence, Co/Al<sub>2</sub>O<sub>3</sub> sample that corresponded to the highest specific area and smallest particle size shifted to mainly C<sub>8</sub>–C<sub>14</sub><sup>+</sup> hydrocarbons fraction. Co/SiC sample enhanced C<sub>9</sub>–C<sub>17</sub> fraction whereas Co/bentonite favoured C<sub>14</sub>–C<sub>25</sub><sup>+</sup> and Co/TiO<sub>2</sub> improved C<sub>16</sub>–C<sub>21</sub><sup>+</sup> fraction. As expected and in agreement to those reported before [11], it can be observed that those catalysts with lower specific area and higher particle size were centred at higher hydrocarbon product distribution. Furthermore, it was important to note that alumina, bentonite and titania supports provided higher amounts of C<sub>21</sub><sup>+</sup> whereas silicon carbide showed negligible amounts of these

hydrocarbons, resulting a very selective catalyst. C<sub>14</sub>–C<sub>20</sub> (centred in C<sub>16</sub>) hydrocarbon fraction could be greatly considered for a diesel formulation. In this sense Co/SiC catalyst not only gave rise to an improvement in the CO conversion and FTS rate, but also afforded an important shift to a higher molecular weight hydrocarbon products distribution rather than Co/Alumina catalyst. Therefore, a study of the promising silicon carbide cobalt based catalyst is still needed in order to shift product distribution to a diesel formulation.

#### 4. Conclusions

A series of cobalt based catalysts supported on alumina, bentonite, titania and silicon carbide were prepared in order to study the effect of support on the Fischer–Tropsch synthesis activity and selectivity. Experiments were carried out in a bench scale fixed bed reactor. TPR results show that Co/TiO<sub>2</sub> and Co/bentonite were easier to reduce than Co/Al<sub>2</sub>O<sub>3</sub> and Co/SiC based catalyst. Particle size depended on nature of support and specific area. Catalytic results indicated that the activity increased in the order of Co/TiO<sub>2</sub> < Co/Al<sub>2</sub>O<sub>3</sub> < Co/bentonite < Co/SiC at temperatures higher than 235 °C. Moreover, catalyst Co/bentonite showed good catalytic activity at low temperatures, although this support enhanced the formation of oxygenated compounds. Hydrocarbon distribution also varied with the support. Co/SiC not only improved CO conversion and FTS rate, but also shifted to higher molecular weight hydrocarbons products distribution than Co/Al<sub>2</sub>O<sub>3</sub>. Moreover, alumina, bentonite and titania supports provided higher amounts of C<sub>21</sub><sup>+</sup> whereas silicon carbide showed negligible amounts of these hydrocarbons, resulting a very selective catalyst.

#### Acknowledgements

Financial Supports from the Ministerio de Industria, Turismo y Comercio of Spain (CENIT-PiIBE project) and ELCOGAS S.A. are gratefully acknowledged.

#### References

- [http://www.ipcc.ch/pdf/assessment-report/ar4/syr/ar4\\_syr.pdf](http://www.ipcc.ch/pdf/assessment-report/ar4/syr/ar4_syr.pdf).
- J. Fermoso, B. Arias, M.V. Gil, M.G. Plaza, C. Pevida, J.J. Pis, F. Rubiera, *Bioresour. Technol.* 101 (2010) 3230–3235.
- A. Demirbas, *Prog. Energy Combust. Sci.* 33 (2007) 1–18.
- M.J.A. Tijmensen, A.P.C. Faaij, C.N. Hamelinck, M.R.M. van Hardeveld, *Biomass Bioenergy* 23 (2002) 129–152.
- G.W. Huber, S. Iborra, A. Corma, *Chem. Rev.* 106 (2006) 4044–4098.
- Ø. Borg, S. Eri, E.A. Blekkan, S. Stosater, H. Wigum, E. Rytter, A. Holmen, *J. Catal.* 248 (2007) 89–100.
- D.B. Bukur, X. Lang, D. Mukesh, W.H. Zimmerman, M.P. Rosynek, C. Li, *Ind. Eng. Chem. Res.* 29 (1990) 1588–1599.
- S.-H. Kang, J.W. Bae, K.-J. Woo, P.S. Sai Prasad, K.-W. Jun, *Fuel Process. Technol.* 91 (2010) 399–403.
- G.L. Bezemer, P.B. Radstakea, U. Falke, H. Oosterbeek, H.P.C.E. Kuipers, A.J. van Dillen, K.P. de Jong, *J. Catal.* 237 (2006) 152–161.
- G.L. Bezemer, J.H. Bitter, H.P.C.E. Kuipers, H. Oosterbeek, J.E. Holeywijn, X. Xu, F. Kapteijn, A.J. van Dillen, K.P. de Jong, *J. Am. Chem. Soc.* 128 (2006) 3956–3964.
- A. Tavasoli, K. Sadaghiani, A. Nakhaei-pour, M. Ghalbi Ahangari, *Iran. J. Chem. Chem. Eng.* 26 (2007) 1–9.
- M.C. Bahome, L.L. Jewell, K. Padayachy, D. Hildebrandt, D. Glasser, A.K. Datye, N.J. Coville, *Appl. Catal. A: Gen.* 328 (2007) 243–251.
- A. Balbo, D. Sciti, A.L. Costa, A. Bellosi, *Mater. Chem. Phys.* 103 (2007) 70–77.
- J.L. Li, N.J. Coville, *Appl. Catal. A: Gen.* 181 (1999) 201–208.
- A.M. Hilmen, D. Schanke, K.F. Hanssen, A. Holmen, *Appl. Catal. A: Gen.* 186 (1999) 169–188.
- R.D. Jones, C.H. Bartholomew, *Appl. Catal.* 39 (1988) 77–88.
- L. Tian, C.F. Huo, D.B. Cao, Y. Yang, J. Xu, B.S. Wu, H.-W. Xiang, Y.-Y. Xu, Y.-W. Li, *J. Mol. Struct. THEOCHEM* 941 (2010) 30–35.
- F.E.M. Farias, F.G. Sales, F.A.N. Fernandes, *J. Nat. Gas Chem.* 17 (2008) 175–178.
- Y. Liu, B.-T. Teng, X.-H. Guo, Y. Li, J. Chang, L. Tian, X. Hao, Y. Wang, H.-W. Xiang, Y.-Y. Xu, Y.-W. Li, *J. Mol. Catal. A: Chem.* 272 (2007) 182–190.
- W. Ngantsoue-Hoc, Y. Zhang, R.J. O'Brien, M. Luo, B.H. Davis, *Appl. Catal. A: Gen.* 236 (2002) 77–89.
- G. Zhao, C. Zhang, S. Qin, H. Xiang, H. Li, *J. Mol. Catal. A: Chem.* 286 (2008) 137–142.

- [22] L. Guzzi, G. Stefler, O. Geszti, Z. Koppány, Z. Kónya, É. Molnár, M. Urbán, I. Kiricsi, *J. Catal.* 244 (2006) 24–32.
- [23] A. Bao, K. Liew, J. Li, *J. Mol. Catal. A: Chem.* 304 (2009) 47–51.
- [24] A. Jean-Marie, A. Griboval-Constant, A.Y. Khodakov, F. Diehl, *Chimie* 12 (2009) 660–667.
- [25] B. Sexton, A. Hughes, T. Turney, *J. Catal.* 97 (1986) 390–406.
- [26] D.A. Wesner, G. Linden, H.B. Bonzel, *Appl. Surf. Sci.* 26 (1986) 335–356.
- [27] S. Eri, J.G. Goodwin Jr., G. Marcelin, T. Riis, US Patent 4,880,763 (1989).
- [28] N. Tien-Thao, M.H. Zahedi-Niaki, H. Alamdari, S. Kaliaguine, *J. Catal.* 245 (2007) 348–357.